Published in final edited form as:
J Neurosurg. 2009 October ; 111(4): 712–723. doi:10.3171/2009.3.JNS081348.

Development of the Wireless Instantaneous Neurotransmitter Concentration System for intraoperative neurochemical monitoring using fast-scan cyclic voltammetry:

Technical note

Jonathan M. Bledsoe, M.D.[1], **Christopher J. Kimble, M.A.**[2], **Daniel P. Covey, B.S.**[3], **Charles D. Blaha, Ph.D.**[4], **Filippo Agnesi, M.S.**[5], **Pedram Mohseni, Ph.D.**[6], **Sidney Whitlock, B.S.**[2], **David M. Johnson, B.S.**[2], **April Horne, B.S., M.B.A.**[2], **Kevin E. Bennet, B.S.Ch.E., M.B.A.**[2], **Kendall H. Lee, M.D., Ph.D.**[1,5], and **Paul A. Garris, Ph.D.**[3]

[1]Department of Neurologic Surgery, Mayo Clinic, Rochester, Minnesota

[2]Division of Engineering, Mayo Clinic, Rochester, Minnesota

[3]Department of Biological Sciences, Illinois State University, Normal, Illinois

[4]Department of Psychology, University of Memphis, Tennessee

[5]Department of Physiology and Biomedical Engineering, Mayo Clinic, Rochester, Minnesota

[6]Department of Electrical Engineering and Computer Science, Case Western Reserve University, Cleveland, Ohio

Abstract

Object—Emerging evidence supports the hypothesis that modulation of specific central neuronal systems contributes to the clinical efficacy of deep brain stimulation (DBS) and motor cortex stimulation (MCS). Real-time monitoring of the neurochemical output of targeted regions may therefore advance functional neurosurgery by, among other goals, providing a strategy for investigation of mechanisms, identification of new candidate neurotransmitters, and chemically guided placement of the stimulating electrode. The authors report the development of a device called the Wireless Instantaneous Neurotransmitter Concentration System (WINCS) for intraoperative neurochemical monitoring during functional neurosurgery. This device supports fast-scan cyclic voltammetry (FSCV) at a carbon-fiber microelectrode (CFM) for real-time, spatially and chemically resolved neurotransmitter measurements in the brain.

Methods—The FSCV study consisted of a triangle wave scanned between −0.4 and 1 V at a rate of 300 V/second and applied at 10 Hz. All voltages were compared with an Ag/AgCl reference electrode. The CFM was constructed by aspirating a single carbon fiber (r = 2.5 μm) into a glass capillary and pulling the capillary to a microscopic tip by using a pipette puller. The exposed carbon

Address correspondence to: Kendall H. Lee, M.D., Ph.D., Department of Neurologic Surgery, Mayo Clinic, 200 First Street Southwest, Rochester, Minnesota 55905. lee.kendall@mayo.edu..

Portions of this work were presented in poster form at the National Institutes of Health Neural Interfaces Conference in Cleveland, Ohio, in July 2008.

Portions of this work were also presented in abstract form at the American Society for Stereotactic and Functional Neurosurgery Biennial Meeting in Vancouver, BC, Canada, on June 4, 2008, and at the American Academy of Neurological Surgery Annual Meeting in Sedona, Arizona, on September 12, 2008.

The authors report no other conflict of interest concerning the materials or methods used in this study or the findings specified in this paper.

fiber (that is, the sensing region) extended beyond the glass insulation by ~ 100 μm. The neurotransmitter dopamine was selected as the analyte for most trials. Proof-of-principle tests included in vitro flow injection and noise analysis, and in vivo measurements in urethane-anesthetized rats by monitoring dopamine release in the striatum following high-frequency electrical stimulation of the medial forebrain bundle. Direct comparisons were made to a conventional hardwired system.

Results—The WINCS, designed in compliance with FDA-recognized consensus standards for medical electrical device safety, consisted of 4 modules: 1) front-end analog circuit for FSCV (that is, current-to-voltage transducer); 2) Bluetooth transceiver; 3) microprocessor; and 4) direct-current battery. A Windows-XP laptop computer running custom software and equipped with a Universal Serial Bus–connected Bluetooth transceiver served as the base station. Computer software directed wireless data acquisition at 100 kilosamples/second and remote control of FSCV operation and adjustable waveform parameters. The WINCS provided reliable, high-fidelity measurements of dopamine and other neurochemicals such as serotonin, norepinephrine, and ascorbic acid by using FSCV at CFM and by flow injection analysis. In rats, the WINCS detected subsecond striatal dopamine release at the implanted sensor during high-frequency stimulation of ascending dopaminergic fibers. Overall, in vitro and in vivo testing demonstrated comparable signals to a conventional hardwired electrochemical system for FSCV. Importantly, the WINCS reduced susceptibility to electromagnetic noise typically found in an operating room setting.

Conclusions—Taken together, these results demonstrate that the WINCS is well suited for intraoperative neurochemical monitoring. It is anticipated that neurotransmitter measurements at an implanted chemical sensor will prove useful for advancing functional neurosurgery.

Keywords

deep brain stimulation; neuromodulation; neurotransmitter; voltammetry; dopamine

FUNCTIONAL neurosurgery has recently gained rapid popularity for its remarkable therapeutic success with a variety of neurological and psychiatric conditions. For example, DBS is used for treating PD, essential tremor, dystonia, and depression,[5,27,28,39,42,43,60] whereas MCS is established for providing relief from chronic pain.[12,57,58] Although the precise mechanism of action of these procedures is not completely understood, emerging evidence supports the hypothesis that modulation of specific central neuronal systems contributes to clinical efficacy. Depending on the targeted site of stimulation, putative neurotransmitters released include dopamine, glutamate, GABA, and adenosine for DBS,[4,26,36–38] and endogenous opioid peptides for MCS.[41] Monitoring the neurochemical output of modulated circuits in humans may therefore advance functional neurosurgery by, among other goals, providing a new strategy for investigation of mechanisms; identification of novel candidate neurotransmitters; chemically guided placement of the stimulating electrode; and development of closed-loop, smart, neural-interface devices.

Microdialysis and voltammetry dominate neurochemical monitoring in experimental animals in vivo.[55,61] Because samples are physically removed from brain tissue by an implanted probe and analyzed externally by sophisticated analytical instrumentation, microdialysis excels in selectivity, sensitivity, and versatility. By contrast, voltammetry uses electrochemistry to detect analytes directly at an implanted microsensor, a strategy affording superior temporal and spatial resolution. Both microdialysis and voltammetry have been used in experiments in rats to test the hypothesis that DBS of the STN releases the neurotransmitter dopamine in the striatum. Albeit controversial, this hypothesis is important, because activation of surviving nigrostriatal dopaminergic neurons may contribute, at least in part, to the clinical efficacy of DBS of the STN for treating PD.[35,51] Whereas microdialysis has experienced difficulty demonstrating an increase in striatal dopamine during HFS of the STN in the rat,[13,45,46,53] voltammetric

microsensors have detected a robust signal that is dependent on current, frequency, and pulse-train duration.[36] Similar to microdialysis, PET has been unable to detect dopamine release in the human striatum with DBS of the STN.[1,56] However, this imaging technique, which indirectly assesses neurotransmitter levels by displacement of a radiolabeled receptor ligand, may not have sufficient sensitivity for investigating the role of dopamine release in neuromodulation.[29]

Although the analytical attributes of voltammetry appear well suited for integrating intraoperative neurochemical monitoring into the functional neurosurgical procedure, there remain significant obstacles to realizing this attractive strategy. These include the following: 1) lack of an FDA-approved device for electrochemical measurements at a microsensor implanted in the brain in humans; 2) susceptibility of conventional electrochemical measurements to ambient noise inherent in the operating room; 3) safety issues related to line-powered devices; and 4) complexities of the functional neurosurgical environment. A possible solution to these obstacles is a small, battery-powered, wireless instrument like those that have been fabricated for voltammetric measurements of neurotransmitter release in freely moving rats.[18,31]

We describe here the development of a new device, called the WINCS, for intraoperative neurochemical monitoring during functional neurosurgery. The WINCS supports FSCV at a CFM, a state-of-the-art electroanalytical technique that was selected for its exquisite temporal, spatial, and chemical resolution.9 Modeled after an instrument used in laboratory rats,24,[25] but designed in compliance with FDA-recognized consensus standards for medical electrical device safety, the WINCS consists of 4 modules: 1) front-end analog circuit for FSCV; 2) Bluetooth transceiver; 3) microprocessor; and 4) direct-current battery. Packaged in a sterilizable enclosure that may be attached to the stereotactic frame, the WINCS is electrically connected to a brain-implanted microsensor and wirelessly linked to a home-base laptop computer for remote control. We report in this study a series of proof-of-principle tests demonstrating that the WINCS is appropriate for intraoperative neurochemical monitoring in support of functional neurosurgery.

Methods

Experimental Animals

Four adult male Sprague-Dawley rats weighing between 300 and 400 g were used for in vivo testing. Rats were housed under standard conditions, with free access to food and water. Care was provided in accordance with National Institute of Health guidelines (publication 86–23) and approved by the Mayo Clinic Institutional Animal Care and Use Committee.

Protocol for FSCV at a CFM

For FSCV, the potential at the CFM was linearly ramped every 0.1 seconds between −0.4 and 1 V at a rate of 300 V/second. The microsensor rested at a bias potential of −0.4 V between scans. The WINCS was compared with a conventional hardwired system, the UEI (Department of Chemistry Electronic Shop, University of North Carolina), which was computer-controlled using commercially available software (ESA Biosciences).[48] The CFM was constructed by aspirating a single carbon fiber (r = 2.5 μm) into a borosilicate glass capillary and pulling it to a microscopic tip by using a pipette puller.14 The Ag/AgCl reference electrode was fabricated by chloridizing a 31-gauge silver wire.23

Flow Injection Analysis

Flow injection analysis was used for in vitro measurements with FSCV at a CFM.[34] In this procedure, which is well established for device testing and microsensor calibration, a CFM is

placed in a flowing stream, and analyte is injected as a bolus. A buffer solution composed of 150 mM sodium chloride and 25 mM HEPES at a pH of 7.4 was pumped across the CFM, which was positioned in the center of the inflow tubing to a Plexiglas reservoir, at a rate of 4 ml/minute. The Ag/AgCl reference electrode was located in the bottom of the reservoir, immersed in buffer solution. An electronic loop injector, locally fabricated, introduced a bolus of analyte for 10 seconds into the flowing stream at defined test concentrations.

In Vivo Experiments

After anesthesia was induced intraperitoneally with 1.6 g/kg urethane, the rats were immobilized in a commercially available stereotactic device (David Kopf Instruments). Multiple craniectomies were performed for implantation of the reference, stimulating, and recording electrodes. Stereotactic coordinates were obtained from a rat brain atlas based on flat-skull position,[54] using the bregma and dura mater as reference points. All coordinates (AP, ML, and DV), are given in millimeters. The stimulating electrode was placed just above the MFB (AP −4.6, ML +1.2, DV −8.0 to −9.0) of the right hemisphere. The recording electrode (that is, the CFM) was positioned ipsilaterally in the dorsomedial striatum (AP +1.2, ML +2.0, DV −4.5 to −6.0). The reference electrode was inserted in superficial cortical tissue contralateral to stimulating and recording electrodes. The positions of the stimulating and recording electrodes were initially adjusted to obtain a robust signal for electrically evoked levels of extracellular dopamine measured in the striatum, and positioning was not changed thereafter for the remainder of the experiment.

Electrical Stimulation

Electrical stimulation was computer generated and consisted of biphasic stimulus pulses (300 μA and 2 msec each phase). The twisted bipolar stimulating electrode (MS 303/2, Plastics One) was insulated except for the exposed tips, which were separated by 1 mm. The 60-Hz pulse trains were applied through a constant-current generator and optical isolator (NL 80, Neurolog; Medical Systems Corp.). In the case of the UEI, but not the WINCS, stimulation pulse trains were synchronized with the voltammetry so that a voltage scan and stimulus pulse never overlapped in time.

Results

Instrument Overview

As shown in Fig. 1A, the WINCS is an external chemical measurement device supporting a microsensor implanted in the brain and wirelessly controlled by a home-base computer. When supporting human intraoperative neurochemical monitoring, the WINCS circuit board and battery (Fig. 1B) will be packaged in a hermetically sealed polycarbonate case (Fig. 1C) that allows sterilization with the Sterrad gas plasma process and will be attached to the stereotactic frame. The home base will be situated remotely to the WINCS, so as not to interfere with the functional neurosurgical procedure, but within wireless transmission distance of an ~ 10-m line of sight.

Hardware Development

The WINCS incorporates modules for the microprocessor; front-end analog circuitry for FSCV; Bluetooth radio; and a battery on a single, battery-powered, multilayer, printed circuit board. The C8051F061 microprocessor (Silicon Laboratories) controls electrochemistry, data acquisition, and wireless communication. A digital-to-analog converter produces the potential applied to the CFM for FSCV; an analog-to-digital converter samples FSCV at a rate of 100 kilosamples/second.

In the front-end analog circuitry for FSCV, an LMV751 low-noise operational amplifier (National Semi-conductor Corp.) acts as a transimpedance amplifier for current-to-voltage conversion. A downstream INA2132U difference amplifier (Texas Instruments, Inc.) subtracts the potential applied to the CFM (that is, the triangular ramp waveform applied during FSCV) prior to signal digitization.

Digital telemetry between the remote unit and the base-station computer uses Bluetooth radio technology. A Universal Serial Bus–connected Bluetooth "dongle" on the base-station computer completes the Bluetooth link. Bluetooth devices operate in the unlicensed Industrial, Scientific, and Medical band of 2.400–2.500 GHz, by using a spread-spectrum, frequency-hopping, full-duplex signal. A rechargeable 740-mAh lithium-polymer battery (Ultralife Batteries, Inc.) was selected as the power source. When fully charged, battery capacity is adequate for at least 3 hours of continuous operation.

The base-station computer is a Windows-XP laptop computer running custom software that controls the parameters and operation of the WINCS, such as starting and stopping data acquisition and transmission, modifying the applied potential waveform, and changing the sampling rate. Data are saved to the computer hard drive as a sequence of unsigned 2-byte integers, a format suitable for postprocessing by software such as MATLAB (The MathWorks, Inc.) or LabVIEW (National Instruments).

Fast–Scan Cyclic Voltammetry at a CFM

The FSCV method specializes in rapid and chemically resolved analyte monitoring at a microsensor.[9,25,55] Like all voltammetric techniques, the FSCV measures electroactive species by applying a voltage to the sensing surface and measuring oxidative and reductive currents. A CFM is the microsensor of choice for FSCV. The size of the sensing region depends on the length of the exposed carbon fiber beyond the glass insulation and its diameter; a carbon-fiber length of ~ 100 μm and a diameter of 5 μm were used for these measurements.

The potential of the CFM is scanned at regular intervals for the FSCV technique. Only during the actual voltage scan is the analyte measured. The scan was applied at 10 Hz (that is, every 100 msec) in this study, and the potential applied to the CFM during a single scan and plotted versus time is shown in Fig. 2A *upper panel*. The duration of the scan is 9.3 msec at the scan rate of 300 V/second. The high scan rate produces a large background current due to double-layer capacitance at the CFM tip. Background current collected in the absence of analyte and during a single scan is shown in Fig. 2A *center panel (black line)* and plotted with time. (Current corresponds to the applied voltage in the triangle scan in the panel above.) The large background current masks additional current due to the presence of dopamine *(red line)*. Fortunately, background current is stable over short times and can be subtracted to reveal the pure faradic current produced by dopamine electrolysis. In the background-subtracted current recording shown in Fig. 2A *lower panel*, the downward-facing peak at ~ 4 msec is due to oxidation of dopamine into dopamine-orthoquinone, and the upward-facing peak at ~ 8 msec is due to the reduction of the electroformed quinone back to dopamine. Times for dopamine oxidation and reduction, extended vertically in Fig. 2A by the *dashed lines*, correspond to the potentials of ~ +0.6 and −0.2 V, respectively (see triangle scan in *upper panel*). The voltammogram, which serves as a chemical signature to identify the analyte detected, is the plot of these measured currents with respect to the applied voltage, rather than time.

As shown in Fig. 2B, background-subtracted cyclic voltammograms can be plotted sequentially by using a pseudocolor display, with time as the x axis, voltage as the y axis, and current as the z or color axis. This pseudocolor plot shows dopamine measured in the striatum of an anesthetized rat and elicited by electrical stimulation of the MFB. Features in the pseudocolor display occurring at ~ 5–10 seconds correspond to the electrically evoked release of dopamine

measured at the CFM tip. Specifically, green-purple features at ~ +0.6 V and black-yellow features at ~ −0.2 V directly relate to the oxidation of dopamine and the reduction of the electroformed quinone, respectively. The brown color reflects zero current, established by the background subtraction procedure.

Dynamic changes in dopamine levels produced by the electrical stimulation are obtained by plotting current measured at the peak oxidative potential for dopamine (~ +0.6 V; *horizontal white line* on the pseudocolor plot in Fig. 2B) with time, as shown in Fig. 2C *upper panel*. Current was converted to concentration by postcalibration of the CFM with flow injection analysis and known dopamine standard solutions. An individual background-subtracted voltammogram can also be obtained for any time point by plotting current measured at the applied potential (*vertical white line* on the pseudocolor plot in Fig. 2B), as shown in Fig. 2C *lower panel*. Note that downward- and upward-facing peaks of the individual background-subtracted voltammogram directly correspond to the green-purple and black-yellow features of the pseudocolor display, respectively. All measurements shown in Fig. 2 were collected at the same CFM.

In Vitro FSCV at a CFM

Figure 3 compares the WINCS to a conventional hardwired system (that is, UEI) for FSCV measurements of dopamine at a CFM by using flow injection analysis. In Fig. 3 *(lower left panel)*, current recorded at the oxidative potential for dopamine (~ +0.6 V) during a 10-second, 10-μM bolus injection is plotted with time. Notice similar dynamics and amplitude for signals collected by the WINCS *(red line)* and the UEI *(black line)*. The small time delay between the bolus injection at 5 seconds and the increase in signal is due to the length of tubing between the reservoir containing the CFM and the upstream injection of dopamine. A similar delay occurs when the bolus injection is terminated. The *upper left panel* shows comparable dopamine background-subtracted cyclic voltammograms generated by the 2 systems from the plateau signal of the bolus injection. The pseudocolor plots shown in Fig. 3 *right* and obtained during the dopamine bolus injection are also similar for the WINCS and the UEI. A slight injection artifact can be observed as a vertical line at 5 and 15 seconds. All measurements were collected at the same CFM.

Figure 4 displays concentration-dependent responses measured with flow injection analysis. Single responses to varying concentrations of dopamine (0.25, 1, 2.5, 5, and 10 μM) and collected at the same CFM by the WINCS are shown in Fig. 4A. Note the increase in current with each increase in dopamine concentration. Background-subtracted cyclic voltammograms collected during the plateau of these responses are shown in Fig. 4B. Also note the increasing size of the oxidative and reductive peaks with increasing dopamine concentration. Figure 4C compares concentration-response curves generated by the WINCS *(open circles)* and the UEI *(solid circles)*. Current was measured at the plateau response and represents the average of triplicate measurements. Both systems recorded a similar linear dependence of measured oxidative current with dopamine concentration. The correlation coefficient (r^2) was 0.994 for the WINCS and 0.977 for the UEI. All measurements were collected at the same CFM. Similar dopamine concentration-response curves were also recorded at 3 additional CFMs for both systems (data not shown).

Sample background-subtracted cyclic voltammograms for different analytes and collected by the WINCS are shown in Fig. 5. These voltammograms, which have been previously described in the literature,[3,30,32] illustrate some of the capabilities of FSCV for resolving chemical signals. These analytes are also considered “interferents” to the voltammetric measurement of dopamine in the brain, because all would contribute to current monitored at the oxidation potential for dopamine if present. Figure 5 panels A, B, and C show voltammograms for 1 μM dopamine, norepinephrine, and serotonin, respectively. Dopamine and norepinephrine,

which differ by a single hydroxyl group on the side chain attached to the catechol ring, give similar voltammograms. In contrast, the voltammogram for the indoleamine serotonin is distinguished from these other two catecholamines by the sharper oxidative peak, and in particular the less-negative reductive peak. Serotonin, because it adsorbs more readily to the CFM surface,[30] also gives more oxidative current than both dopamine and norepinephrine at the same concentration. Similarly, dopamine provides slightly more oxidative current than norepinephrine.

Figure 5 panels D, E, and F compare voltammograms for 200 μM ascorbic acid, an acidic pH change, and a basic pH change, respectively. All 3 of these, as well as the dopamine metabolites homovanillic acid and 3,4-dihydroxyphenylacetic acid,[3] can be readily distinguished from dopamine. Ascorbic acid, which is found in high (0.5 mM) concentrations in the brain, has been considered the primary interferent to the voltammetric determination of dopamine.[55] Brain pH, which changes as a result of altered neuronal activity, is also a key interferent for monitoring dopamine with FSCV in vivo.

In Vivo FSCV at a CFM

The electrically evoked release of dopamine in the striatum of urethane-anesthetized rats was used to compare FSCV measurements collected by the WINCS and UEI in vivo. Recordings shown in Fig. 6A were collected at the same CFM and striatal location during MFB stimulation with a high-frequency (60 Hz), 2-second pulse train delivered at 5 seconds. The increase in dopamine levels during the stimulation reflects exocytotic neurotransmitter release elicited by action potentials, which are activated when electrical current is applied to ascending dopaminergic fibers in the MFB, and arrive at the dopaminergic terminals in the striatum.[64] The return of dopamine levels to baseline is due to the action of the dopamine transporter, which translocates released dopamine back into the dopaminergic terminal in the process of neuronal uptake. Note the similar kinetics of the evoked response recorded by the WINCS and the UEI, and background-subtracted dopamine voltammograms generated by the 2 systems (Fig. 6B).

As shown in Fig. 6C, pseudocolor displays describing the evoked recordings are also quite similar for the 2 systems. Note that the UEI has slightly lower noise levels than the WINCS, which shows a more wavy appearance of the brown background in the pseudocolor plot. There is also an additional feature in the WINCS plot *(upper panel)* near the reductive current for dopamine. This feature reflects stimulus artifact, and it will appear randomly in the pseudocolor display during the stimulation period because pulse trains were not synchronized to the voltage scan in this device. No stimulus artifact is observed in the UEI recording *(lower panel)*, because this system generated both the voltage scan and the stimulus pulses, and synchronizes the 2 so that they are not applied at the same time. Nevertheless, the stimulus artifact did not interfere with the evoked recording and voltammogram collected by the WINCS and shown in Fig. 5A and B, respectively. The effect of pulse-train duration (0.5, 1, 2, and 4 seconds) on evoked dopamine responses recorded by the WINCS is shown in Fig. 5D. These recordings, demonstrating an increase in extracellular dopamine levels with train duration, were collected at the same CFM and location in the striatum. None of the responses was distorted by stimulus artifact. Comparable results were obtained in 3 additional rats (data not shown).

In Vitro Noise Analysis

To evaluate susceptibility to electromagnetic interference, “dry” measurements collected by the WINCS and UEI were compared in an operating room for large-animal surgeries. A dummy cell, a simple resistor-capacitor circuit mimicking the electrical properties of a CFM, was connected to each system, and they were placed on the surgical table within 2 feet of each other. Various electrical devices normally used during functional neurosurgery were turned on

and off sequentially to evaluate noise perturbations. Figure 7 *left* shows measured current at what would be the typical dopamine oxidative potential (0.6 V) at a CFM with respect to time for the WINCS and UEI. Pseudocolor plots for these same recordings are shown for the WINCS and UEI in Fig. 7 *right*. In the operating room test, noise levels of the WINCS were lower than those of the UEI. Increased noise levels recorded by the UEI are indicated by the larger peak-to-peak amplitude of baseline current and the wavy features in the pseudocolor plot. Moreover, powering the trephine drill and cauterizing unit, and hand waving over the dummy cell all caused distortion in the current trace and pseudocolor plot for the UEI, whereas the WINCS was largely unaffected. Drill powering caused the greatest distortion. Little distortion was recorded in either system by turning on surgical lights or powering the anesthesia equipment.

Discussion

We describe the development of the WINCS for intraoperative neurochemical monitoring during functional neurosurgery. The WINCS is wireless technology supporting FSCV at a CFM for temporally, spatially, and chemically resolved measurements of neurotransmitters. Direct comparisons made across a series of in vitro and in vivo proof-of-principle tests demonstrated that the WINCS compared favorably to an established, research-grade hardwired system. Most importantly, the WINCS exhibited less susceptibility to ambient electrical noise in a typical operating room setting. Taken together, these results demonstrate the utility of the WINCS for supporting future chemical measurements at a microsensor implanted in the human brain.

Development of the WINCS

The WINCS is modeled after instrumentation called RAT, which was developed for chemical measurements in experimental animals.[24,25] The rationale for RAT was to replace the wire tether linking animal and recording equipment to allow more natural behavior and reduce movement artifact from cable micromotion. Both RAT and the WINCS use a modular structure of front-end circuitry for FSCV; Bluetooth digital telemetry; microprocessor; and battery. However, several improvements to the RAT design have been implemented in the WINCS, including the following: 1) a newer microprocessor with greater analog-to-digital converter bit resolution, more internal memory, and faster clock speed; 2) wirelessly programmable waveform parameters (scan bias, range, and rate) and offset; 3) a higher-precision voltage reference for the microprocessor; 4) a more advanced Bluetooth module; 5) low-power mode to preserve battery life when idle; 6) battery voltage sensing and low-power alert; and 7) a longer-lasting battery. Most importantly and unlike RAT, the WINCS was designed in compliance with FDA-recognized consensus standards for medical electrical device safety.

To our knowledge, although microdialysis has been applied to the human brain,[20] chemical measurements taken directly at an implanted microsensor have not. One key limitation is lack of an FDA-approved potentiostat to support in situ electrochemistry. Several key criteria must be met to develop such instrumentation. Foremost are patient safety, signal fidelity, and integration with the existing functional neurosurgical setup. Advantageous design features of the WINCS, a small, wireless, sterilizable, battery-powered unit, meet these criteria. For example, the low-power battery minimizes risk of electrical shock through a wall-powered connection. The WINCS is also easily attached to the stereotactic frame and transmits data to a remotely located base station, and thus does not contribute to crowding in the busy space surrounding the patient. Finally, signal quality of the WINCS is enhanced by measurement digitization near the point of acquisition. Combined with digital telemetry of the recorded signal, these characteristics provide the WINCS an enhanced immunity to ambient noise. Indeed, we show that the WINCS is capable of performing with high fidelity in the electromagnetically noisy environment inside a typical operating room, and that it is superior

to a research-grade hardwired system. The WINCS should be similarly proficient in an operating room for functional human neurosurgery.

The one disadvantage exhibited by the WINCS was distortion of the pseudocolor plot by stimulus artifact (Fig. 6C *upper panel*). This distortion is not due to any design flaw, but rather is related to the lack of synchrony between FSCV voltage scans applied to the CFM and the externally generated electrical pulses applied to the implanted stimulating electrode. Indeed, no artifact is observed with the UEI, simply because the software controls both the voltage scan and stimulus pulse, and avoids overlap by synchronizing the two. Although the stimulus artifact recorded in the pseudocolor plot did not interfere with time-dependent monitoring of dopamine or obtaining an individual voltammogram for dopamine (Fig. 6A and B), there are ready solutions available if distortion becomes an issue. For example, the WINCS and its home-base system could be reprogrammed to input a trigger from the stimulus generator, and could use this signal to synchronize voltage scan and electrical pulse. Designing the WINCS with a dedicated module for stimulus generation, as was done with RAT,[25] is a further option.

The WINCS and Neuromodulation

Although the clinical efficacy of DBS and MCS is unchallenged,[5,27,28,40,42,43,60] the mechanism of action of these functional neurosurgical procedures is incompletely understood and quite controversial. Deep brain stimulation is perhaps more widely studied in this regard. Because DBS and the lesioning surgeries of subthalamotomy, pallidotomy, and thalamotomy are effective in the same regions for treating the motor disorders of PD, dystonia, and essential tremor, respectively, stimulation-evoked silencing of pathologically hyperactive neurons was initially postulated as the primary mechanism.[6,7,52] This notion was further supported by early work measuring electrophysiological characteristics in humans[19] and animal models,[8] although stimulus artifact prevented recording during pulse application. However, more recent evidence suggests that DBS action is far more complex, and that it may involve additional mechanisms, including excitation and stimulus-pulse entrainment of neuronal cell bodies at the target site[2,22,62] as well as activation of afferents and efferents and fibers of passage coursing through.[44] Collectively, these actions could normalize the activity of structures within the basal ganglia complex associated with motor deficits by an anti-oscillatory action.[47]

An additional and related hypothesis emerging is that neuromodulation releases neurotransmitters locally at the target site and within interconnected pathways.[35] The utility of the WINCS device described herein and the concept of intraoperative neurochemical monitoring during functional neurosurgery, in general, are based on this neurotransmitter release hypothesis. On the one hand, it is both reasonable and intuitive to submit that electrical stimulation of the brain releases neurotransmitters. Consistent with this general rule and depending on the targeted site, the putative neurotransmitters released include dopamine, glutamate, GABA, and adenosine for DBS,[4,26,36–38] and endogenous opioid peptides for MCS.[41] On the other hand, the pertinent question is what role, if any, does neurotransmitter release play in the mechanism of clinically effective neuromodulation? Additional research is thus needed to address this critical question, and the new device described in this study is proposed to permit such inquiry in clinical and experimental studies.

By supporting real-time chemical measurements at an implanted microsensor, the WINCS affords a powerful research tool in the investigation of DBS central mechanisms. Deep brain stimulation of the STN serves as an instructive case study, because this neuromodulation procedure has been investigated in laboratory animals by using both microdialysis and voltammetry, and in humans by using PET studies to test the neurotransmitter release hypothesis. The DBS of the STN potentially elicits neurotransmitter release in several loci within the basal ganglia.

One possibility we are pursuing with the WINCS is that DBS of the STN for the treatment of PD activates surviving nigrostriatal dopaminergic neurons in the following ways: 1) direct stimulation of dopaminergic axons coursing near the STN; 2) stimulation of STN glutamatergic efferents projecting to the SNc, the locus of cell bodies for nigrostriatal dopaminergic neurons; and 3) stimulation of STN glutamatergic efferents projecting to the pedunculopontine tegmental nucleus and subsequent activation of excitatory glutamatergic and cholinergic neurons innervating the SNc.[35]

The notion that DBS of the STN evokes striatal dopamine release is admittedly controversial and is opposed by some clinical and preclinical studies.[15,51] Indeed, DBS of the STN does not increase dopamine release in patients with PD, as measured by PET scanning[1,29,56] or in most microdialysis studies in which intact or 6-hydroxydopamine–lesioned rats, a widely used animal model of PD, have been tested.45،46،53 The one exception is Bruet et al.,13 who collected dialysate in 6-hydroxydopamine–lesioned rats in a striatal location between the severely denervated (~ 80%) lateral aspect and the intact medial region, suggesting that the lesion's degree of sampled tissue was similar to the preclinical phase of PD. However, DBS of the STN is most effective in parkinsonian patients who respond well to levodopa,[11] and is even contraindicated for patients who do not respond to this biochemical precursor to dopamine (and the predominant drug prescribed for treating PD),33 suggesting a role for endogenous dopamine production. Also consistent with activation of dopaminergic neurons is a reduction or even elimination of levodopa dose with DBS of the STN,49،50 and the finding that this treatment elicits dyskinesias resembling excess levodopa,39 and impulsivity, a dopamine-related behavior.[21]

The difficulty microdialysis has with detecting dopamine release during STN stimulation may be due to the large probe size (~ 300-μm tip diameter; compare with 5 μm for the CFM used in this study), which is associated with damage to surrounding tissue.[16] A consequence of this perturbation is that a CFM positioned immediately adjacent to the dialysis probe was unable to detect MFB-evoked dopamine release in the rat striatum, yet an identical sensor positioned at a distance of 1 mm away concurrently measured ~ 10 μM dopamine.10 Thus, STN stimulation may not be able to elicit detectable dopamine levels in the damaged tissue surrounding the probe for monitoring by microdialysis. Consistent with this conjecture is the finding that administration of nomifensine, a dopamine uptake inhibitor, or pargyline, a monoamine oxidase inhibitor, increases dialysate dopamine levels in the striatum to detectable levels following HFS of the STN,45 perhaps by permitting more dopamine released in the distal undamaged tissue to diffuse into the damaged area and subsequently be sampled by the probe.10 The sensitivity of current PET scans may also be insufficient to detect dopamine release after DBS of the STN.[29] These results suggest that the voltammetric microsensor approach with the WINCS may be more suitable than conventional microdialysis or PET scanning for characterizing striatal dopamine levels during DBS of the STN.

Preliminary studies by our group in which HFS of the STN was used in anesthetized rats support the utility of the WINCS and voltammetry for intraoperative neurochemical monitoring. For example, HFS of the STN elicited a robust signal measured with amperometry, another real-time electroanalytical technique, at a CFM implanted in the intact rat striatum.[36] This signal was dependent on the current, frequency, and pulse-train duration of HFS, and was pharmacologically identified as dopamine. Moreover, after electrophysiologically identifying the STN trajectory and positioning the stimulating electrode at these stereotactic coordinates, HFS reliably evoked dopamine release in the intact rat striatum as measured by FSCV at a CFM.[17] Voltammograms collected in the striatum and evoked by HFS of the STN were both consistent with dopamine and identical to those also recorded in this region at the same CFM, but evoked by HFS of the MFB or SNc. It should be noted that although dopamine measurements have proven problematic, microdialysis has been able to record increases in the

extracellular levels of pallidal and nigral glutamate and nigral GABA levels with DBS of the STN.[63] The globus pallidus and substantia nigra are output targets of the STN. The caveat is that dialysate levels of glutamate and GABA may not originate from exocytotic neurotransmitter release,[59] but this issue could be addressed by WINCS-based biosensor measurements.

In addition to investigations of mechanisms of action, another potentially exciting application of the WINCS is neurochemically guided implantation of the stimulating electrode during functional neurosurgery. For example, if the neurotransmitter release hypothesis of neuromodulation is substantiated and specific targets underlying clinical efficacy are positively identified, then chemical signals collected by the WINCS at an implanted microsensor could serve as a feedback signal for not only localizing, but also fine-tuning electrode placement. It thus may be possible to use the WINCS to improve the precision of the functional neurosurgical approach. Substituting neurochemical monitoring for electrophysiological recording to verify the stimulating electrode trajectory obtained by MR imaging of the patient's brain is also conceivable.

Future Directions

Future work further developing the WINCS concept will take 3 immediate directions. The first is to expand device functionality to accommodate amperometric biosensors and bioelectric microelectrodes. The second is to establish proof of concept for WINCS-based intraoperative neurochemical monitoring, using a large-animal model for mock functional neurosurgery to mimic critical features of the human neuromodulation approach. The third is development of human- and WINCS-compatible microsensors.

Conclusions

We propose the WINCS as a multipurpose chemical measurement instrument to support intraoperative neurochemical monitoring during functional neurosurgery. By providing temporally and chemically resolved measurements at an implanted microsensor in targeted brain regions and in regions up- and downstream to the activated site, the WINCS should be beneficial by providing chemical feedback regarding the efficacy of the targeted site for neuromodulation, thus driving more precise placement of the therapeutic stimulating electrode. The WINCS could also be used to investigate the neuromodulation mechanism of action in the human brain, potentially identifying new candidate neurotransmitters, and ultimately it could form the basis for development of a closed-loop, smart, neural-interface device for maintaining optimal neurotransmitter levels in real time.

Acknowledgments

The authors acknowledge Andy Alexander, Robert Ensman, John Poehlman, and George Rebec for their development of the RAT device, on which the WINCS was modeled.

Disclosure This work was supported by the following entities: National Science Foundation (Grant Nos. DBI-0138011 and DBI-0754615 to Dr. Garris), National Institutes of Health (Grant No. K08 NS 52232), Mayo Foundation (2008–2010 Research Early Career Development Award for Clinician Scientists to Dr. Lee), and Mathews Foundation (John T. and Lillian Mathews Professorship in Neuroscience).

Abbreviations used in this paper

AP	anteroposterior
CFM	carbon-fiber microelectrode
DBS	deep brain stimulation

DV	dorsoventral
FSCV	fast-scan cyclic voltammetry
GABA	γ-aminobutyric acid
HFS	high-frequency stimulation
MCS	motor cortex stimulation
MFB	medial forebrain bundle
ML	mediolateral
PD	Parkinson disease
RAT	Real-Time Animal Telemetry
SNc	substantia nigra pars compacta
STN	subthalamic nucleus
UEI	Universal Electrochemistry Instrument
WINCS	Wireless Instantaneous Neurotransmitter Concentration System

References

1. Abosch A, Kapur S, Lang AE, Hussey D, Sime E, Miyasaki J, et al. Stimulation of the subthalamic nucleus in Parkinson's disease does not produce striatal dopamine release. Neurosurgery 2003;53:1095–1105. [PubMed: 14580276]
2. Bar-Gad I, Elias S, Vaadia E, Bergman H. Complex locking rather than complete cessation of neuronal activity in the globus pallidus of a 1-methyl-4-phenyl-1,2,3,6-tetrahydropyridine-treated primate in response to pallidal microstimulation. J Neurosci 2004;24:7410–7419. [PubMed: 15317866]
3. Baur JE, Kristensen EW, May LJ, Wiedmann DJ, Wightman RM. Fast-scan voltammetry of biogenic amines. Anal Chem 1988;60:1268–1272. [PubMed: 3213946]
4. Bekar L, Libionka W, Tian GF, Xu Q, Torres A, Wang X, et al. Adenosine is crucial for deep brain stimulation-mediated attenuation of tremor. Nat Med 2008;14:75–80. [PubMed: 18157140]
5. Benabid AL. Deep brain stimulation for Parkinson's disease. Curr Opin Neurobiol 2003;13:696–706. [PubMed: 14662371]
6. Benabid AL, Pollak P, Louveau A, Henry S, de Rougemont J. Combined (thalamotomy and stimulation) stereotactic surgery of the VIM thalamic nucleus for bilateral Parkinson disease. Appl Neurophysiol 1987;50:344–346. [PubMed: 3329873]
7. Bergman H, Wichmann T, DeLong MR. Reversal of experimental parkinsonism by lesions of the subthalamic nucleus. Science 1990;249:1436–1438. [PubMed: 2402638]
8. Beurrier C, Bioulac B, Audin J, Hammond C. High-frequency stimulation produces a transient blockade of voltage-gated currents in subthalamic neurons. J Neurophysiol 2001;85:1351–1356. [PubMed: 11287459]
9. Borland, LM.; Michael, AC. An introduction to electrochemical methods in neuroscience. In: Borland, LM.; Michael, AC., editors. Electrochemical Methods for Neuroscience. CRC Press; Boca Raton, FL: 2007. p. 1-15.
10. Borland LM, Shi G, Yang H, Michael AC. Voltammetric study of extracellular dopamine near microdialysis probes acutely implanted in the striatum of the anesthetized rat. J Neurosci Methods 2005;146:149–158. [PubMed: 15975664]
11. Breit S, Schulz JB, Benabid AL. Deep brain stimulation. Cell Tissue Res 2004;318:275–288. [PubMed: 15322914]
12. Brown JA, Pilitsis JG. Motor cortex stimulation for central and neuropathic facial pain: a prospective study of 10 patients and observations of enhanced sensory and motor function during stimulation. Neurosurgery 2005;56:290–297. [PubMed: 15670377]

13. Bruet N, Windels F, Bertrand A, Feuerstein C, Poupard A, Savasta M. High frequency stimulation of the subthalamic nucleus increases the extracellular contents of striatal dopamine in normal and partially dopaminergic denervated rats. J Neuropathol Exp Neurol 2001;60:15–24. [PubMed: 11202172]

14. Cahill PS, Walker QD, Finnegan JM, Mickelson GE, Travis ER, Wightman RM. Microelectrodes for the measurement of catecholamines in biological systems. Anal Chem 1996;68:3180–3186. [PubMed: 8797378]

15. Chang JY, Shi LH, Luo F, Zhang WM, Woodward DJ. Studies of the neural mechanisms of deep brain stimulation in rodent models of Parkinson's disease. Neurosci Biobehav Rev 2008;32:352–366. [PubMed: 18035416]

16. Clapp-Lilly KL, Roberts RC, Duffy LK, Irons KP, Hu Y, Drew KL. An ultrastructural analysis of tissue surrounding a microdialysis probe. J Neurosci Methods 1999;90:129–142. [PubMed: 10513596]

17. Covey, DP.; Ramsson, ES.; Heidenreich, BA.; Blaha, CD.; Lee, KH.; Garris, PA. Monitoring subthalamic nucleus-evoked dopamine release in the rat striatum using fast-scan cyclic voltammetry in vivo. In: Phillips, PEM.; Sandberg, SG.; Ahn, S., et al., editors. Monitoring Molecules in Neuroscience; Proceedings of the 12th International Conference on In Vivo Methods; Vancouver: University of British Columbia Institute of Mental Health; 2008. p. 398-400.

18. Crespi F, Dalessandro D, Annovazzi-Lodi V, Heidbreder C, Norgia M. In vivo voltammetry: from wire to wireless measurements. J Neurosci Methods 2004;140:153–161. [PubMed: 15589345]

19. Dostrovsky JO, Levy R, Wu JP, Hutchison WD, Tasker RR, Lozano AM. Microstimulation-induced inhibition of neuronal firing in human globus pallidus. J Neurophysiol 2000;84:570–574. [PubMed: 10899228]

20. Fedele E, Mazzone P, Stefani A, Bassi A, Ansaldo MA, Raiteri M, et al. Microdialysis in Parkinsonian patient basal ganglia: acute apomorphine-induced clinical and electrophysiological effects not paralleled by changes in the release of neuroactive amino acids. Exp Neurol 2001;167:356–365. [PubMed: 11161624]

21. Frank MJ, Samanta J, Moustafa AA, Sherman SJ. Hold your horses: impulsivity, deep brain stimulation, and medication in parkinsonism. Science 2007;318:1309–1312. [PubMed: 17962524]

22. Garcia L, Audin J, D'Alessandro G, Bjoulac B, Hammond C. Dual effect of high-frequency stimulation on subthalamic neuron activity. J Neurosci 2003;23:8743–8751. [PubMed: 14507974]

23. Garris PA, Christensen JR, Rebec GV, Wightman RM. Real-time measurement of electrically evoked extracellular dopamine in the striatum of freely moving rats. J Neurochem 1997;68:152–161. [PubMed: 8978721]

24. Garris PA, Ensman R, Poehlman J, Alexander A, Langley PE, Sandberg SG, et al. Wireless transmission of fast-scan cyclic voltammetry at a carbon-fiber microelectrode: proof of principle. J Neurosci Methods 2004;140:103–115. [PubMed: 15589340]

25. Garris, PA.; Greco, PG.; Sandberg, SG.; Howes, G.; Pongmaytegul, S.; Heidenreich, BA., et al. In vivo voltammetry with telemetry. In: Michael, AC.; Borland, LM., editors. Electrochemical Methods for Neuroscience. CRC Press; Boca Raton, FL: 2007. p. 233-259.

26. Garris PA, Walker QD, Wightman RM. Dopamine release and uptake rates both decrease in the partially denervated striatum in proportion to the loss of dopamine terminals. Brain Res 1997;753:225–234. [PubMed: 9125407]

27. Greene P. Deep-brain stimulation for generalized dystonia. N Engl J Med 2005;352:498–500. [PubMed: 15689590]

28. Hardesty DE, Sackeim HA. Deep brain stimulation in movement and psychiatric disorders. Biol Psychiatry 2007;61:831–835. [PubMed: 17126303]

29. Hilker R, Voges J, Ghaemi M, Lehrke R, Rudolf J, Koulousakis A, et al. Deep brain stimulation of the subthalamic nucleus does not increase the striatal dopamine concentration in parkinsonian humans. Mov Disord 2003;18:41–48. [PubMed: 12518299]

30. Jackson BP, Dietz SM, Wightman RM. Fast-scan cyclic voltammetry of 5-hydroxytryptamine. Anal Chem 1995;67:1115–1120. [PubMed: 7717525]

31. Kagohashi M, Nakazato T, Yoshimi K, Moizumi S, Hattori N, Kitazawa S, et al. Wireless voltammetry recording in unanesthetised behaving rats. Neurosci Res 2008;60:120–127. [PubMed: 17983679]

32. Kawagoe KT, Garris PA, Wightman RM. pH-Dependent processes at Nafion-coated carbon-fiber microelectrodes. J Electroanal Chem 1993;359:193–197.
33. Kern DS, Kumar R. Deep brain stimulation. Neurologist 2007;13:237–252. [PubMed: 17848864]
34. Kristensen EW, Wilson RM, Wightman RM. Dispersion in flow injection analysis measured with microvoltammetric electrodes. Anal Chem 1986;58:986–988.
35. Lee KH, Blaha CD, Garris PA, Mohseni P, Horne AE, Bennet KE, et al. Evolution of deep brain stimulation: human electrometer and smart devices supporting the next generation of therapy. Neuromodulation. 2009 [in press].
36. Lee KH, Blaha CD, Harris BT, Cooper S, Hitti FL, Leiter JC, et al. Dopamine efflux in the rat striatum evoked by electrical stimulation of the subthalamic nucleus: potential mechanism of action in Parkinson's disease. Eur J Neurosci 2006;23:1005–1014. [PubMed: 16519665]
37. Lee KH, Chang SY, Roberts DW, Kim U. Neurotransmitter release from high-frequency stimulation of the subthalamic nucleus. J Neurosurg 2004;101:511–517. [PubMed: 15352610]
38. Lee KH, Kristic K, van Hoff R, Hitti FL, Blaha CD, Harris B, et al. High-frequency stimulation of the subthalamic nucleus increases glutamate in the subthalamic nucleus of rats as demonstrated by in vivo enzyme-linked glutamate sensor. Brain Res 2007;1162:121–129. [PubMed: 17618941]
39. Limousin P, Krack P, Pollak P, Benazzous A, Ardouin C, Hoffman D, et al. Electrical stimulation of the subthalamic nucleus in advanced Parkinson's disease. N Engl J Med 1998;339:1105–1111. [PubMed: 9770557]
40. Lozano AM, Mayberg HS, Giacobbe P, Hamani C, Craddock RC, Kennedy SH. Subcallosal cingulate gyrus deep brain stimulation for treatment-resistant depression. Biol Psychiatry 2008;64:461–467. [PubMed: 18639234]
41. Maarrawi J, Peyron R, Mertens P, Costes N, Magnin M, Sindou M, et al. Motor cortex stimulation for pain control induces changes in the endogenous opioid system. Neurology 2007;69:827–834. [PubMed: 17724284]
42. Mayberg HS, Lozano AM, Voon V, McNeely HE, Seminowicz D, Hamani C, et al. Deep brain stimulation for treatment-resistant depression. Neuron 2005;45:651–660. [PubMed: 15748841]
43. Mazzone P, Lozano A, Stanzione P, Galati S, Scarnati E, Peppe A, et al. Implantation of human pedunculopontine nucleus: a safe and clinically relevant target in Parkinson's disease. Neuroreport 2005;16:1877–1881. [PubMed: 16272871]
44. McIntyre CC, Savasta M, Kerkerian-Le Goff L, Vitek JL. Uncovering the mechanism(s) of action of deep brain stimulation: activation, inhibition, or both. Clin Neurophysiol 2004;115:1239–1248. [PubMed: 15134690]
45. Meissner W, Harnack D, Paul G, Reum T, Sohr R, Morgenstern R, et al. Deep brain stimulation of subthalamic neurons increases striatal dopamine metabolism and induces contralateral circling in freely moving 6-hydroxydopamine-lesioned rats. Neurosci Lett 2002;328:105–108. [PubMed: 12133566]
46. Meissner W, Reum T, Paul G, Harnack D, Sohr R, Morgenstern R, et al. Striatal dopaminergic metabolism is increased by deep brain stimulation of the subthalamic nucleus in 6-hydroxydopamine lesioned rats. Neurosci Lett 2001;303:165–168. [PubMed: 11323111]
47. Meissner W, Schreiter D, Volkmann J, Trottenberg T, Schnieder GH, Sturm V, et al. Deep brain stimulation in late stage Parkinson's disease: a retrospective cost analysis in Germany. J Neurol 2005;252:218–223. [PubMed: 15729530]
48. Michael DJ, Joseph JD, Kilpatrick MR, Travis ER, Wightman RM. Improving data acquisition for fast-scan cyclic voltammetry. Anal Chem 1999;71:3941–3947. [PubMed: 10500480]
49. Molinuevo JL, Valldeoriola F, Tolosa E, Rumia J, Valls-Sole J, Roldan H, et al. Levodopa withdrawal after bilateral subthalamic nucleus stimulation in advanced Parkinson disease. Arch Neurol 2000;57:983–988. [PubMed: 10891980]
50. Moro E, Scerrati M, Romito LM, Roselli R, Tonali P, Albanese A. Chronic subthalamic nucleus stimulation reduces medication requirements in Parkinson's disease. Neurology 1999;53:85–90. [PubMed: 10408541]
51. Moyer JT, Wolf JA, Finkel LH. Effects of dopaminergic modulation on the integrative properties of the ventral striatal medium spiny neuron. J Neurophysiol 2007;98:3731–3748. [PubMed: 17913980]

52. Patel NK, Heywood P, O'Sullivan K, McCarter R, Love S, Gill SS. Unilateral subthalamotomy in the treatment of Parkinson's disease. Brain 2003;126:1136–1145. [PubMed: 12690053]

53. Paul G, Reum T, Meissner W, Marburger A, Sohr R, Morgenstern R, et al. High frequency stimulation of the subthalamic nucleus influences striatal dopaminergic metabolism in the naive rat. Neuroreport 2000;11:441–444. [PubMed: 10718291]

54. Paxinos, G.; Watson, C. The Rat Brain in Stereotaxic Coordinates. Vol. ed 2. Academic Press; New York: 1986.

55. Robinson DL, Hermans A, Seipel AT, Wightman RM. Monitoring rapid chemical communication in the brain. Chem Rev 2008;108:2554–2584. [PubMed: 18576692]

56. Thobois S, Fraix V, Savasta M, Costes N, Pollak P, Mertens P, et al. Chronic subthalamic nucleus stimulation and striatal D2 dopamine receptors in Parkinson's disease—a [(11)C]-raclopride PET study. J Neurol 2003;250:1219–1223. [PubMed: 14586606]

57. Tsubokawa T, Katayama Y, Yamamoto T, Hirayama T, Koyama S. Chronic motor cortex stimulation for the treatment of central pain. Acta Neurochir Suppl (Wien) 1991;52:137–139. [PubMed: 1792954]

58. Tsubokawa T, Katayama Y, Yamamoto T, Hirayama T, Koyama S. Chronic motor cortex stimulation in patients with thalamic pain. J Neurosurg 1993;78:393–401. [PubMed: 8433140]

59. van der Zeyden M, Oldenziel WH, Rea K, Cremers TI, Westerink BH. Microdialysis of GABA and glutamate: analysis, interpretation and comparison with microsensors. Pharmacol Biochem Behav 2008;90:135–147. [PubMed: 17939932]

60. Volkmann J. Deep brain stimulation for the treatment of Parkinson's disease. J Clin Neurophysiol 2004;21:6–17. [PubMed: 15097290]

61. Watson CJ, Venton BJ, Kennedy RT. In vivo measurements of neurotransmitters by microdialysis sampling. Anal Chem 2006;78:1391–1399. [PubMed: 16570388]

62. Welter ML, Houeto JL, Bonnet AM, Bejjani PB, Mesnage V, Dormont D, et al. Effects of high-frequency stimulation on subthalamic neuronal activity in parkinsonian patients. Arch Neurol 2004;61:89–96. [PubMed: 14732625]

63. Windels F, Bruet N, Poupard A, Urbain N, Chouvet G, Feuerstein C, et al. Effects of high frequency stimulation of subthalamic nucleus on extracellular glutamate and GABA in substantia nigra and globus pallidus in the normal rat. Eur J Neurosci 2000;12:4141–4146. [PubMed: 11069610]

64. Wu Q, Reith ME, Wightman RM, Kawagoe, Garris PA. Determination of release and uptake parameters from electrically evoked dopamine dynamics measured by real-time voltammetry. J Neurosci Methods 2001;112:119–133. [PubMed: 11716947]

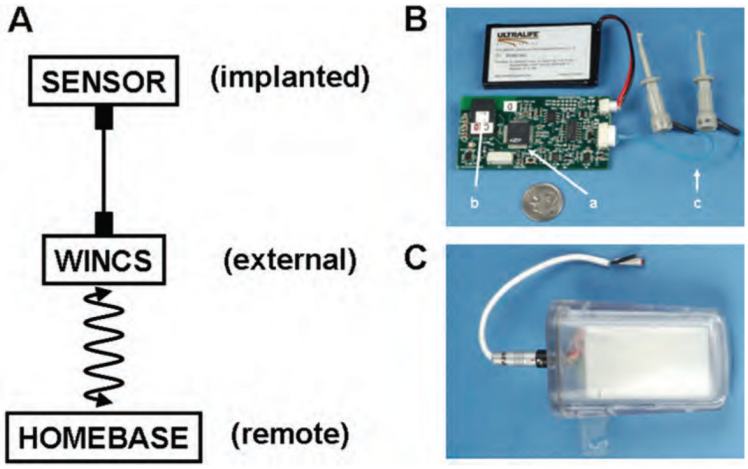

Fig. 1.

The WINCS instrument. A: Conceptual view of the WINCS application. B: Photograph of the WINCS circuit board with attached Ultralife battery (a, microprocessor; b, Bluetooth transceiver; c, leads for working electrode and reference electrodes). C: Photograph of encapsulated WINCS with external electrode contacts.

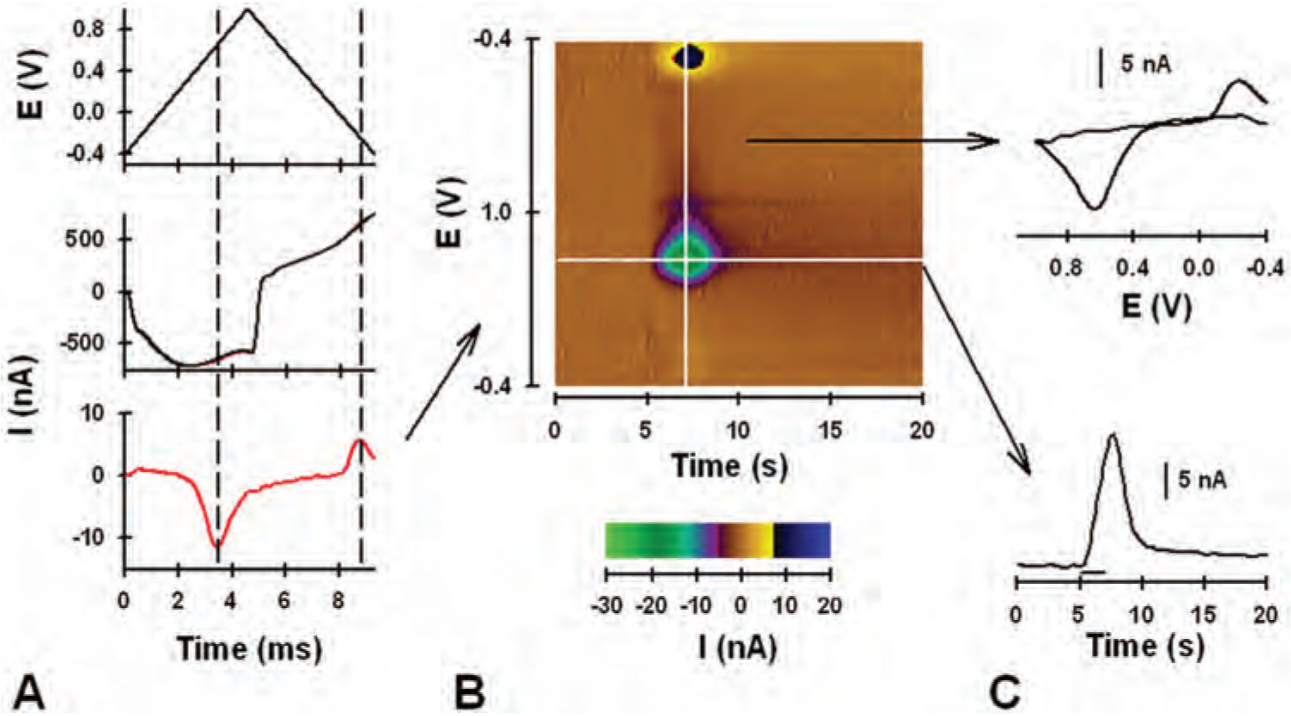

Fig. 2.

Graphs and pseudocolor plot showing results of FSCV. A: Applied triangle waveform *(upper panel)*; background current with *(red line)* and without *(black line)* dopamine (*center panel;* note that the black line overlaps the red line); background-subtracted current *(lower panel)*. B: Pseudocolor plot. C: Background-subtracted cyclic voltammogram *(upper panel)* and current measured at the peak oxidative potential for dopamine and plotted with time *(lower panel)*.

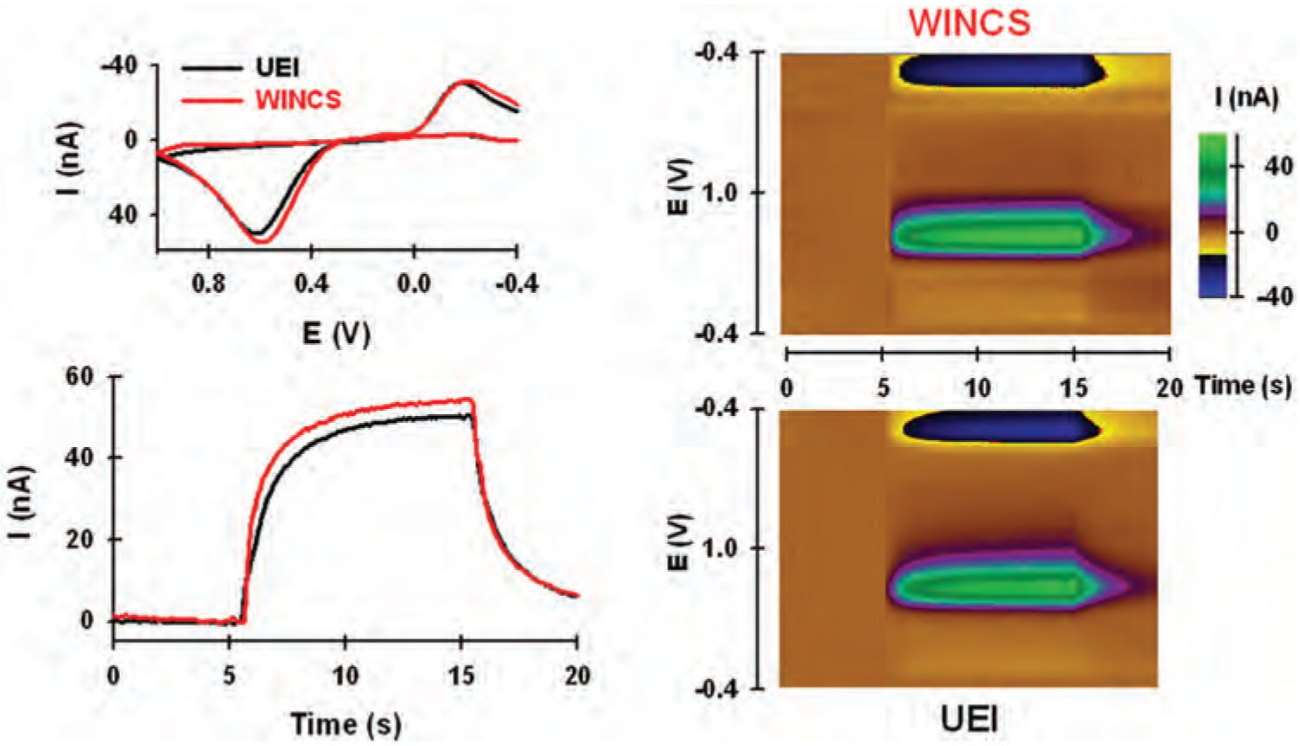

Fig. 3.

Comparison of the WINCS and UEI by using flow injection analysis. *Left*: Background-subtracted voltammograms for dopamine recorded by WINCS and UEI *(upper panel)* and current measured at the peak oxidative potential for dopamine, plotted with time and measured by the WINCS and UEI *(lower panel)*. *Right:* Pseudocolor plots for dopamine determined by testing with the WINCS *(upper panel)* and the UEI *(lower panel)*.

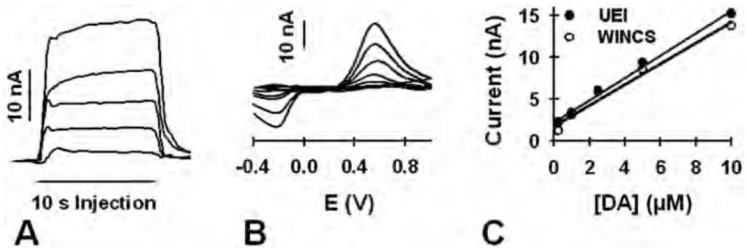

Fig. 4.

Graphs showing comparisons of the WINCS and the UEI for obtaining a dopamine (DA) calibration curve. A: Current measured at the peak oxidative potential for a bolus injection of dopamine and measured by the WINCS. Increasing current corresponds to increasing dopamine concentration (0.25, 1, 2.5, 5, and 10 μM). B: Background-subtracted voltammograms determined by the WINCS. As in panel A, increasing current corresponds to increasing dopamine concentration. C: Dopamine calibration curves collected by the WINCS *(open circles)* and the UEI *(closed circles)*. The line describes the best linear fit.

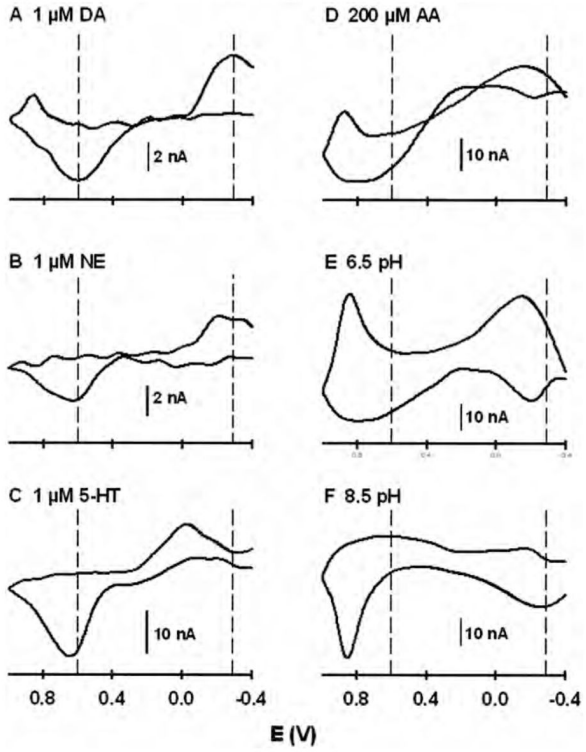

Fig. 5.

Comparison of background-subtracted cyclic voltammograms for different analytes: 1 μM dopamine (A); 1 μM norepinephrine (B); 1 μM serotonin (C); 200 μM ascorbic acid (D); acidic pH change (6.5 pH, E); and basic pH change (8.5 pH, F). AA = ascorbic acid; DA = dopamine; NE = norepinephrine; 5-HT = serotonin.

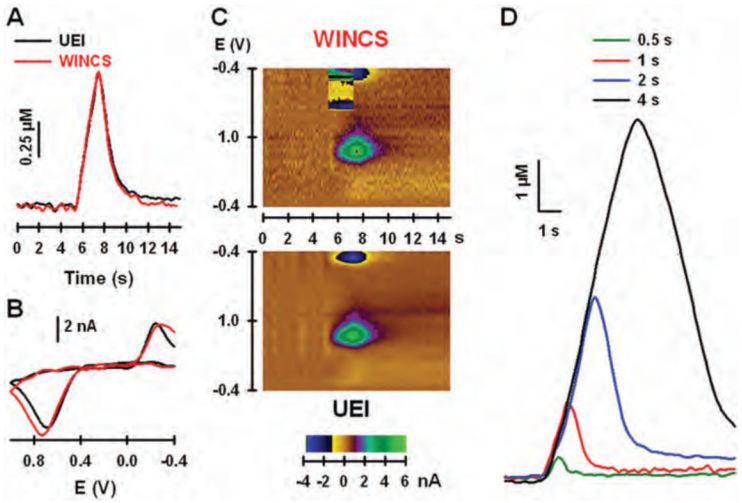

Fig. 6.

In vivo comparison of the WINCS and UEI. A: Electrically evoked dopamine levels measured in the striatum by testing with the WINCS and the UEI. B: Background-subtracted cyclic voltammograms measured by the WINCS and the UEI. C: Pseudocolor plots measured by the WINCS *(upper panel)* and the UEI *(lower panel)*. D: Electrically evoked dopamine levels measured in the striatum by the WINCS and elicited by pulse trains of different duration.

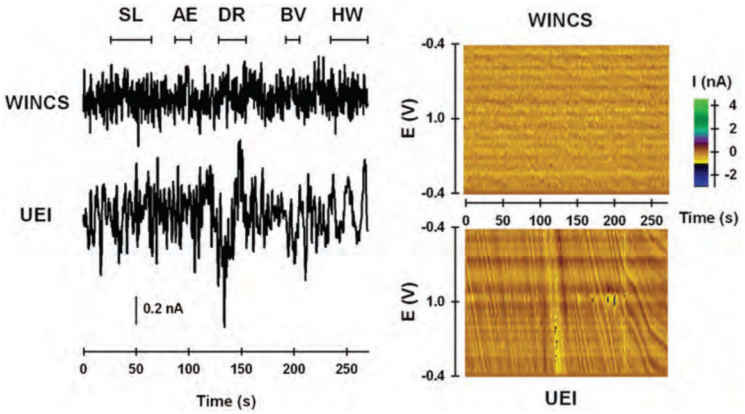

Fig. 7.

Noise analysis comparison of the WINCS and the UEI in large-animal operating room. *Left:* Current measured at a typical oxidative potential (0.6 V) for dopamine, plotted with time, and monitored by the WINCS and the UEI. *Right:* Pseudocolor plots measured by the WINCS and the UEI. AE = anesthesia equipment; BV = “Bovie” cauterization unit; DR = trephine drill; HW = hand waving; SL = surgical lights.